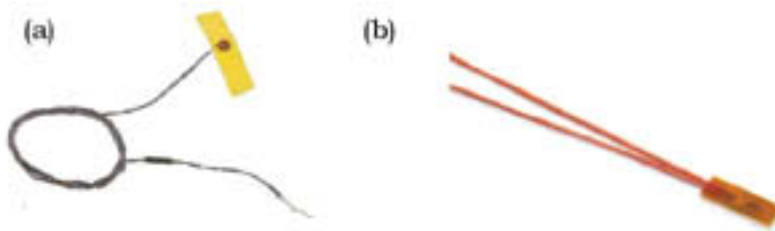


## Sensors

### Thermocouples

Thermocouples base their temperature measurement properties on the reverse of the Peltier effect, the Seebeck effect (see above). Depending on the semiconductors used, different kinds of thermocouples (E, J, K, R, S and T) are commercially available and present different linearities, precisions and transient responses. Although a J or T thermocouple could have provided somehow better precision measures, K-type (Chromel-Alumel) thermocouples were chosen for their low price, universality and high availability. Thereafter, with the introduction of the Pt100 sensor, the acquisition and setup of either J- or T-type thermocouples was dismissed. Planar adhesive K-type thermocouples, with a  $\text{Ø}7$  mm metallic plate for surface measurements were bought (*Lab Facility*) and their interweaved wire-pair was RF-shielded with a cylindrical  $\text{Ø}3$  mm metallic mesh. Thermocouples were then connected to cold-junction compensation circuitry (see p.156), software calibrated by immersion in a hot-water bath (see p.310) and software linearized (see p.312) according to NIST standards.



**Figure 174** - Planar surface thermocouple (a) and thin-film Pt100 RTD (b).

### Pt100 RTD

To attain better temperature resolution, a thin-film class-A calibrated 1/10DIN 5 mm long Pt100 ( $\pm 0.01$  °C precision) was acquired (*Kosmon*). To obtain better response times and more reliable surface temperature measurements, the protecting Teflon sheath of the laminar probe was removed and the probe firmly attached to the Peltier cell surface by physical clamping onto 340 Heat-sink compound (*Dow Corning*) (see p.183). The two probe wire pairs, encased in Teflon, were RF-isolated with a  $\text{Ø}3$  mm cylindrical metallic mesh and connected to a 4-wire resistance reading circuitry (see p.157). The Pt100 probe was then software calibrated by immersion in a hot-water bath (see p. 310) and software linearized (see p. 312) using DIN standard reverse polynomials.

### 8.3.4. SENSOR CALIBRATION

#### Temperature-sensor calibration

In the development of PCR-chip systems, temperature control plays an essential role, and a very important aspect of temperature control lies in the correct calibration of the temperature sensors that will drive the control circuitry. This need is quite acute in PCR systems, where deviations beyond the  $\pm 0.5$  °C range may render otherwise satisfactory PCR experiments completely non-functional or highly diminish their efficiency.

#### *Passive PCR-chip sensor calibration*

The main sensors used in passive PCR-chips were first type-K Ni-Cr surface thermocouples ( $\pm 1$  °C, Ø7 mm metallic base) and then class-A 1/10DIN  $\pm 0.01$  °C Pt100 resistors (see p.309). Although both these sensors were superficial temperature sensors, direct calibration with surface temperature measurements is a quite cumbersome issue. Therefore, the sensors were calibrated by immersion in milliQ water with other commercial reference sensors. Calibration was carried out by software, adjusting the gain of the received amplified sensor signal close to the linear slope of reference sensors, after a linearization stage for both types of sensor had been carried out by software LUTs. Main reference measures were taken at room and water boiling point temperatures, together with slow cooling and heating ramp measures to detect either hysteresis or non-linear behavior. Sensor calibration was repeated regularly every two-months or whenever PCR functional problems came up, in order to dismiss temperature control as the cause of such flaws. Table 25, shown below, is the result of one of these routine calibration assays, using an auto-calibrated  $\pm 0.6$  °C CheckTemp immersion thermometer (*Hanna Instruments*), a immersion K-type thermocouple probe (*Lab Facility*), a class-A 1/10-DIN reference Pt100 RTD (*Kosmon*) and a standard laboratory mercury thermometer (*S. Brannan & Sons*) as reference temperature sensors. Reference temperature was assessed as the mean value of the most precise reference sensors and all measurements were carried out by full immersion of the calibrated sensors, bond together with KPT-1 1/4 (25 mm) polyimide heat resistant tape (*Kapton*) to the commercial reference sensors and placed at the center of a water-filled Pyrex glass warmed with a Series 1000 hotplate stirrer (*Jenway*).

Surface Pt100	Surface thermocouple	CheckTemp Immersion thermometer	Immersion thermocouple	Reference Pt100	Mercury thermometer	Setup
22.3		23.1	22.1	22.3		Ambient (Air)
21.4		22.2	21.5	21.5	21.6	Ambient (Immersion)
21.4		22.1	21.6	21.4	21.6	Ambient (Immersion)
28.8	28.6	29.1	29.2	28.9	29.0	Slow heating
48.5		49.0	48.4	48.3	48.7	Slow heating
99.8		99.2	99.8	99.6	98.6	Boiling point
68.4		68.4	68.4	68.4	68.0	Slow cooling
69.9		70.1	70.2	69.9	69.4	Slow cooling
56.4		57.0	56.6	56.4		Slow cooling
99.9	99.9	99.7	100.0	99.8		Boiling point (stirring)
99.9		99.6	100.2	99.9		Boiling point (stirring)
22.9		23.1	23.1	23.2		Ambient (Air)

**Table 25** - Calibration by immersion of the Pt100 and thermocouple sensors against four different reference temperature sensors. Since the thermocouple was only used at this stage for room temperature control and crosscheck, it was re-calibrated by inferring its slope only at two points.

The reference class-A 1/10DIN Pt100 sensor was monitored with a calibrated 2700 Multi-meter Data Acquisition System (*Keithley*), giving a nominal  $\pm 0.1$  °C error, while the immersion thermocouple was monitored with a 89IV True RMS Multi-meter (*Fluke*), yielding an estimated  $\pm 0.5$  °C error. Therefore, data from these two sensors was used to provide a mean reference temperature value to calculate the mean square error of the calibrated surface Pt100 probe, which, in Table 25, is about 0.019 °C (see Figure 175a).

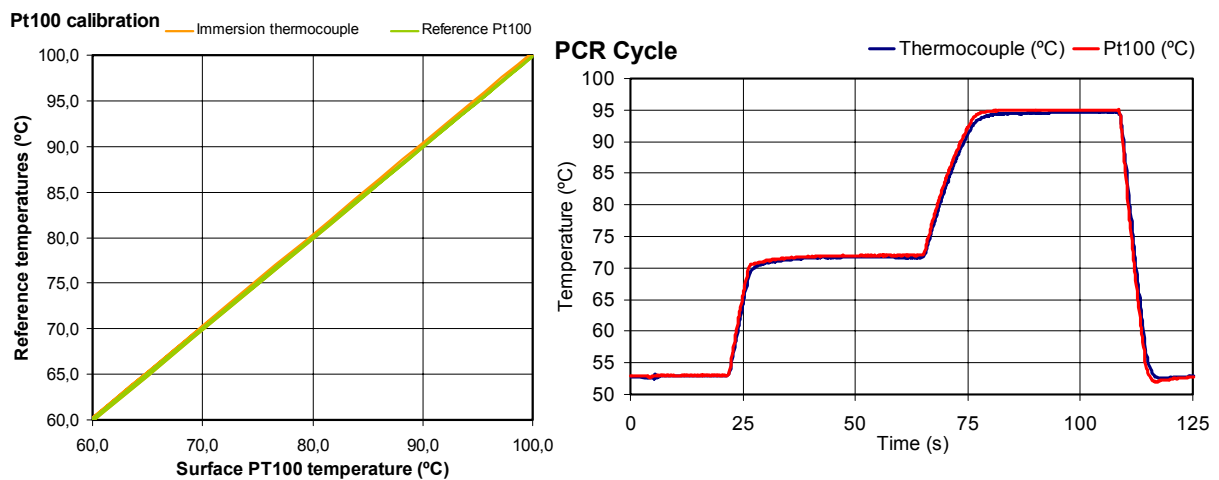


**Figure 175** - Pt100 calibration plot against the two precision temperature sensors (a) and crosscheck of thermocouple and Pt100 surface measurements during operation.

### Crosscheck

After calibration, behavior of surface sensors was crosschecked by evaluating their simultaneous dynamic response to standard PCR cycles on anti-parallel positions at the Peltier cell surface, as illustrated in Figure 175b. These results were also crosschecked by concurrent surface temperature monitoring with a  $\pm 1$  °C Mini-surface Thermometer (*Testo*).

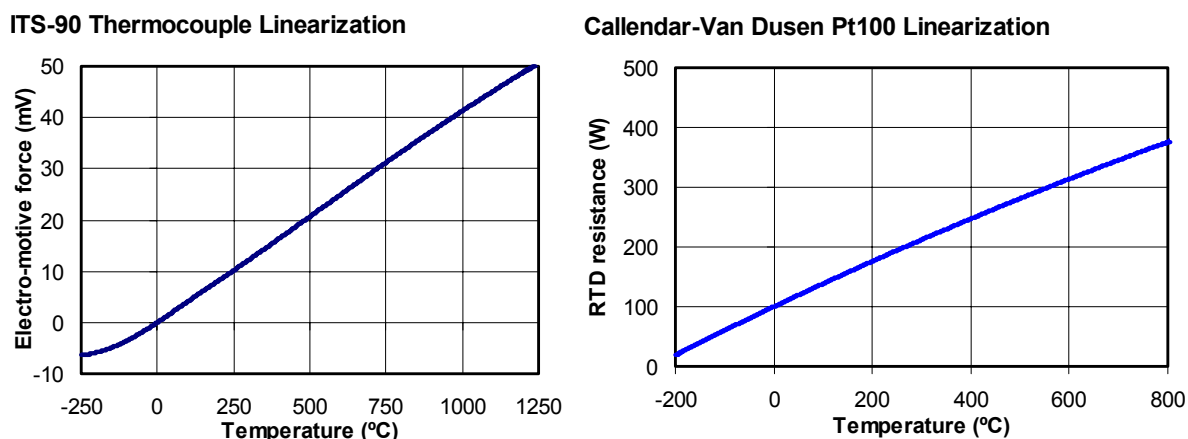


**Figure 176** - Linearization graphs for thermocouple and Pt100 sensors.

### Linearization

As mentioned above, both thermocouple and Pt100 input present small non-linear characteristics and, therefore, they had to be linearized prior to their calibration. This was done using standard ITS-90 Thermocouple Inverse Polynomials for type K thermocouples (see Figure 176a) and a *Callendar-Van Dusen* equation-fitting standard 20<sup>th</sup> order polynomial (see Figure 176b) for the Pt100 RTD.

### **Active PCR-chip integrated-sensor calibration**

Calibration of the developed polysilicon integrated-sensor of active PCR-chips was carried out by immersing the active PCR-chip in a mineral oil solution on a Series 1000 hotplate-stirrer (*Jenway*), together with previously calibrated (see p.310) Pt100 and thermocouple sensors and an external reference thermocouple sensor. The switch from previously used (see p.310) de-ionized water to mineral oil was carried out in order to prevent the occurrence of possible superficial current leakages between contact pads. During calibration, the chip was electrically contacted with electrically-insulated crocodile 2 mm-contact pincers (*Multi Contact*). The

measured integrated-sensor resistance and Pt100/thermocouple temperatures were software-recorded, producing calibration plots as the one shown in Figure 177, whilst the reference temperature provided by the external thermocouple was monitored with a 89IV True-RMS multi-meter (*Fluke*).

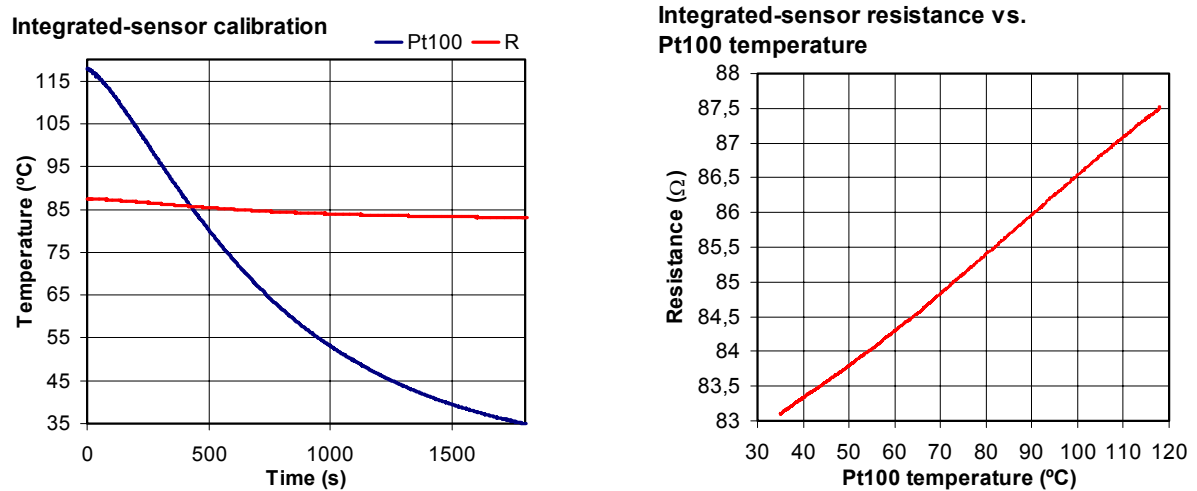


**Figure 177** - Calibration time-dependent (a) and correlation (b) plots for a wafer-B chip. The high linearity of the integrated-sensor readings can be appreciated against the linear interpolation line (red) of the correlation plot. Mean error: 0.0998 Ω.

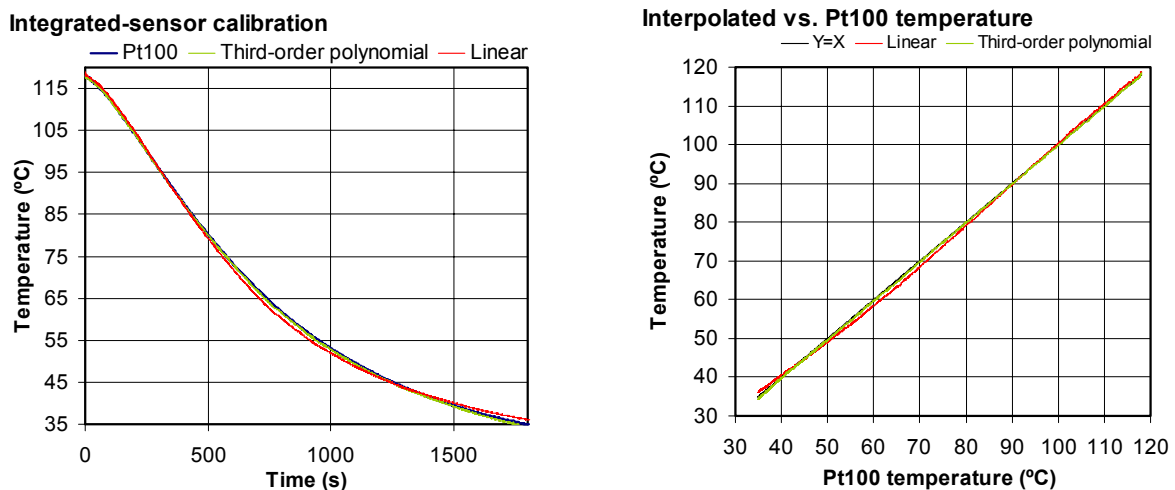


**Figure 178** - Linear and polynomial read-resistance-based temperature interpolation. The mean error for the linear interpolation (0.834 °C) is reduced by the third-order polynomial interpolation down to 0.217 °C, ensuring a maximum mean temperature deviation of ±0.3 °C for the integrated-sensor active chips.

**Linearization**

Even though the linearity of the polysilicon integrated-sensor was greater than expected, a third-order polynomial approximation was calculated using a small custom-built LabView routine. The error committed by third-order and linear polynomial fits was then gauged with interpolated data, as shown in Figure 178. The third-order polynomial fit was then used as a software LUT for real-time interpolation of temperature values.

---

**8.4. SIMULATIONS**

The simulations here reported were conducted on Unix-based SunRay (Sun Microsystems) workstations, with the DESSIS-ISE (*Integrated Systems Engineering*) simulation package. DESSIS-ISE is a powerful tool for thermoelectrical device simulation, since it renders together 2D standard mesh physical analysis and SPICE generated circuit nets, providing the means for the functional (in-circuit) test of simulated devices. Conversely, the main drawback of the DESSIS-ISE system is that it does not provide modules for liquid and air convection simulation. Therefore, in the simulations here reported, PCR reagents (liquid) and air were simulated as solid elements, introducing their respective parameters (relative permittivity, thermal capacity and thermal conductivity), but without accounting for convection effects, which are outstanding contributors to air and liquid thermal behavior. Consequently, simulation results were not realistic in their predictions of heat distribution and transfer in and across the PCR reservoir. Nevertheless, even though the conditions on the PCR-sample could not be accurately assessed, simulation results still provided much functional information on polysilicon resistor behavior, and this information was subsequently and successfully used in the careful design of integrated active PCR-chips (see p.223-225).

**8.4.1. SIMULATION SETUP**

The basic setup and process flow for simulation with DESSIS-ISE is illustrated in Figure 179a. Firstly, a 2D view of the desired device is drawn with MDRAW CAD software (see Figure 179b). Special contact pads for the polysilicon resistor are also drawn and labeled for ulterior netlisting. After design completion, MDRAW generates a boundary file (boundary\_mdr.bnd) and a complete file detailing mesh and doping user-defined parameters

(command\_mdr.cmd). Afterwards, adaptive meshing for different layer thickness can be defined in MDRAW. Typically, three to four mesh-refining levels were used in the simulations here reported, yielding a total of about 10,000 mesh elements. After mesh generation, MDRAW produces two output files: grid\_mdr.grd and doping\_mdr.dat, that will be used by the DESSIS simulation core. The user then defines two additional files. On the one hand, command\_des.cmd includes the circuit SPICE model, its netlist and its input stimulation patterns. On the other hand, parameter.par contains the relevant physical constants of all the materials included in the MDRAW design. After simulation, the DESSIS core produces three output files. A log file (output\_des.log) can be used to trace the simulation, whilst the other two output files (current\_des.plt and plot\_des.dat) are plot files of the simulation results that can be viewed with either Picasso (fixed-time plot) or Inspect (time plot) display software.

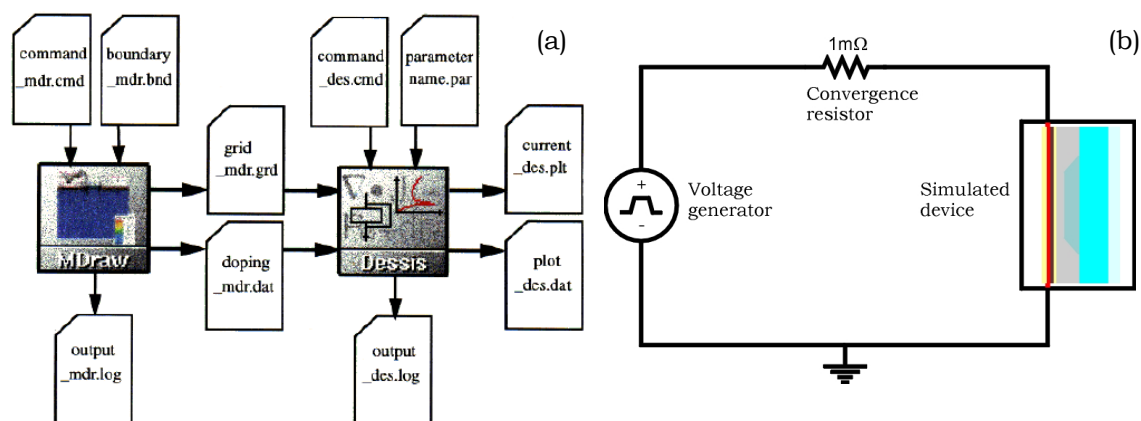


**Figure 179** - Schematic of the basic simulation architecture and flow of the DESSIS-ISE package.

## 8.5. STERILIZATION AND WASHING

Sterilization and washing procedures are of the utmost importance when dealing with such a capricious and delicate reaction as PCR amplification. As already detailed (see p.82), PCR efficiency can be hindered by many inhibitors or its results get easily clouded by contaminating DNA. Additionally, when examining adsorption phenomena on chip walls, methods had to be devised to obtain reproducible experimentation protocols, (i.e. rendering the surface to its original hydrophobic properties after each assay). Moreover, although not being fundamental, the availability of sterilization procedures is of relative import during characterization (that is, prior to batch production), to optimize the number

of chips used, and can also become important for product distribution and manufacture (see p.268).

## **Sterilization**

### ***Conventional sterilization***

Conventional UV light sterilization was routinely carried out prior to mix preparation in all PCR experiments (see p.322). In addition, sterilization by insulation with 260 nm UV light for 30 min was also carried out for all the instrumentation used in PCR-chip experiments: pipettes, syringes, Allen screwdrivers, toric joints, methacrilate devices, etc.

### ***Autoclave sterilization***

Sterilization by UV irradiation is a well-described method ([Sarkar1990a], [Sarkar1990b], [Ou1991], [Sarkar1993]) for surface and small-volume liquid sterilization. Unfortunately, in closed PCR-chips this method cannot be used, since UV light does not effectively permeate through glass or silicon. Therefore, some other method for chip sterilization was required if chips were to be effectively reused. Microbial sterilization can be accomplished with exposition to ethylene oxide (C<sub>2</sub>H<sub>4</sub>O), Freon (HCFC) or carbon dioxide (CO<sub>2</sub>) flow, but this method is unreliable for free-floating DNA chains. On the other hand, the addition of strong acid or base solutions can easily denature free DNA molecules, but might not be adequate to eliminate the toughest bacteria if the concentration is kept low enough to prevent chip corrosion. A great advantage of the here developed silicon-glass anodic bonded chips over alternative methods is that they can be easily autoclaved to render sterile chips after each use. The autoclave protocols for chip sterilization described below were defined, tested and routinely used for chip reutilization, without observing any deterioration on the autoclaved chips.

### **Chip autoclave protocol**

Prior to entering the autoclave, chips were enveloped in a 0.2 mm-thick aluminum film. Afterwards, they were inserted in a 118-LRV autoclave (*Matachana*) and left at 2.2Bar and 135 °C for 15 min. The autoclave was left to cool overnight and a vacuum exhaust step was carried out prior to chip extraction.

## **Washing**

Chip washing was a basic prerequisite for PCR-chip reuse and validation of adsorption phenomena, as it was a necessary step for reuse of electrophoresis chips. Methacrilate devices for high-pressure positive and vacuum pumping (see p.128, p.298) were developed to provide the necessary physical conditions for thorough chip cleansing, since they could be readily coupled to the available N<sub>2</sub>, air, de-ionized water or vacuum sources through Ø4 mm tubing.

### ***Standard washing***

The standard washing protocol, typically followed by chip autoclaving, was the routine chip cleansing methodology between succeeding PCR experiments. De-ionized 18.2 mΩ non-sterile water was directly tapped from CNM-IMB clean-room facilities and injected to the chip through a Ø4 mm tube coupled to the clamping methacrilate device. Water was left to flow for 5 min and, afterwards, 3.5bar N<sub>2</sub> flow (also tapped from CNM-IMB clean-room facilities) was delivered to the chip for 2 min using the same tubing. Finally, the chip was left to dry facedown (lying on the glass cap) on a Series 1000 hotplate-stirrer (*Jenway*) at 150 °C for 10 min. It must be noted here a variation of the standard washing protocol, with the addition of an organic detergent rinse, rendered the chips incompatible with further PCR operation. The cause of this malfunctioning was thought to be the lasting presence of organic detergent residues, which have been frequently described as Taq polymerase inhibitors [Rolf's 1992].

### ***Astringent washing***

To achieve reproducible conditions for Taq polymerase and DNA adsorption to chip walls evaluation, an astringent cleansing protocol (see Table 26) was adapted from the literature [Jönsson 1982] in order to render the SiO<sub>2</sub> surface to its original hydrophobic conditions. Essentially, a three-step rinsing was carried out with an acid solution (37% ACS-ISO hydrochloric acid (*Pancreac*) diluted in stabilized ultra-pure 30% p/v H<sub>2</sub>O<sub>2</sub> (*Pancreac*) and de-ionized H<sub>2</sub>O [1:1:5]), a basic one (30% ACS-ISO ammonia (*Pancreac*) again diluted in H<sub>2</sub>O<sub>2</sub>+H<sub>2</sub>O [1:1:5]) and 96% v/v ultra-pure ethanol (*Pancreac*). When not tapping a clean-room source, constant flow was attained with an adapted Ø8 mm silicone tubing peristaltic pump (*Watson & Marlow*). Non-

### 318 - Technological materials and methods

sterile de-ionized water and N<sub>2</sub> flows were inserted between the different solution rinses to avoid cross-reactions.

<b>Solution</b>	<b>Condition</b>	<b>Source</b>	<b>Time</b>
De-ionized water	Flow	Clean-room tap	2 min
HCl+H <sub>2</sub> O <sub>2</sub> +H <sub>2</sub> O (1:1:5)	Flow	Peristaltic pump	4 min
HCl+H <sub>2</sub> O <sub>2</sub> +H <sub>2</sub> O (1:1:5)	Still	None	1 min
De-ionized water	Flow	Clean-room tap	1 min
N <sub>2</sub>	3.5bar flow	Clean-room tap	30 s
NH <sub>3</sub> +H <sub>2</sub> O <sub>2</sub> +H <sub>2</sub> O (1:1:5)	Flow	Peristaltic pump	4 min
NH <sub>3</sub> +H <sub>2</sub> O <sub>2</sub> +H <sub>2</sub> O (1:1:5)	Still	None	1 min
De-ionized water	Flow	Clean-room tap	1 min
N <sub>2</sub>	3.5bar flow	Clean-room tap	30 s
Ethanol	Flow	Peristaltic pump	4 min
Ethanol	Still	None	1 min
De-ionized water	Flow	Clean-room tap	2 min
N <sub>2</sub>	3.5bar flow	Clean-room tap	2 min
None	Heat dry (150 °C)	Hotplate	10 min

**Table 26** - Astringent chip cleansing protocol. All procedures were carried out at room temperature except where otherwise noted.

---